Plant Molecular Biology (2022) 108:65–76
https://doi.org/10.1007/s11103-021-01222-z

NtCycB2 negatively regulates tobacco glandular trichome formation, exudate accumulation, and aphid resistance

Zhaojun Wang[1] · Xiaoxiao Yan[1] · Hongying Zhang[1] · Ying Meng[1] · Yang Pan[1] · Hong Cui[1]

Received: 9 May 2021 / Accepted: 18 November 2021 / Published online: 26 November 2021

Abstract

Key message ***NtCycB2*** **negatively regulates the initiation of tobacco long stalk glandular trichomes and influences the expression of diterpenoid biosynthesis- and environmental stress resistance-related genes.**

Abstract Many asterid plants possess multicellular trichomes on their surface, both glandular and non-glandular. The *CycB2* gene plays a key role in multicellular trichome initiation, but has distinct effects on different types of trichomes; its mechanisms remain unknown. In tomato (*Solanum lycopersicum*), *SlCycB2* negatively regulates non-glandular trichome formation, but its effects on glandular trichomes are ambiguous. In this study, we cloned the *SlCycB2* homolog of *Nicotiana tabacum*, *NtCycB2*, and analyzed its effect on three types of trichomes, long stalk glandular trichomes (LGT), short stalk glandular trichomes (SGT), and non-glandular trichomes (NGT). Knocking out *NtCycB2* (NtCycB2-KO) promoted LGT formation, while overexpression of *NtCycB2* (NtCycB2-OE) decreased LGT density. SGT and NGT were not significantly influenced in either NtCycB2-KO or NtCycB2-OE plants, indicating that *NtCycB2* regulated only LGT formation in tobacco. In addition, compared with NtCycB2-OE and control plants, NtCycB2-KO plants produced more trichome exudates, including diterpenoids and sugar esters, and exhibited stronger aphid resistance. To further elucidate the function of *NtCycB2*, RNA-Seq analysis of the NtCycB2-KO, NtCycB2-OE, and control plants was conducted. 2,552 and 1,933 differentially expressed genes (DEGs) were found in NtCycB2-KO and NtCycB2-OE plants, respectively. Gene Ontology analysis of the common DEGs revealed that ion transport, carbohydrate and amino acid metabolism, photosynthesis, and transcription regulation processes were significantly enriched. Among these DEGs, diterpenoid biosynthesis genes were upregulated in NtCycB2-KO plants and downregulated in NtCycB2-OE plants. Two MYB transcription factors and several stress resistance-related genes were also identified, suggesting they may participate in regulating LGT formation and aphid resistance.

Keywords *NtCycB2* · Glandular trichome · Aphid resistance · Transcriptome · *Nicotiana tabacum*

Abbreviations

DEG	Differentially expressed gene
GC–MS	Gas chromatography–mass spectrometry
LGT	Long stalk glandular trichomes
NGT	Non-glandular trichomes
qRT-PCR	Quantitative real time PCR
SGT	Short stalk glandular trichomes

Introduction

Plant trichomes are hair-like tissues that develop from aerial epidermal cells and can be found on many plant species. Trichomes vary in shape, size, metabolism, and secretion ability, and may be unicellular or multicellular, glandular or non-glandular (Huchelmann et al. 2017). Trichomes play an important role in response to biotic stress, as they act as a physical barrier against herbivores. Moreover, glandular trichomes can synthesize, store, and secrete large amounts of exudates, including alkaloids, polysaccharides, terpenoids, polyphenols, organic acids, and defensive proteins. In turn, these exudates can entrap or poison herbivores and prevent pathogen infection (Huchelmann et al. 2017; Alain 2018). In addition, trichomes provide protection against abiotic stressors, such as UV–B radiation, drought, and high temperatures (Karabourniotis et al. 1995, 2019).

✉ Hong Cui
cuihong@henau.edu.cn

[1] College of tobacco science, Henan Agricultural University, 63 Nongye Road, Zhengzhou 450002, China

As trichomes are easily accessed, and their development is precisely controlled, they are considered an excellent model for studying the molecular mechanisms involved in controlling plant cell division and differentiation (Yang and Ye 2013). In *Arabidopsis*, which is covered by unicellular non-glandular trichomes, the regulatory network controlling trichome initiation and development has been extensively studied, and many regulatory genes have been identified. These genes include *GLABRA1* (*GL1*), which encodes an R2R3 MYB transcription factor, *GLABRA3* (*GL3*) and its homolog *ENHANCER OF GL3* (*EGL3*), which encode basic helix-loop-helix (bHLH) transcription factors, and *TRANSPARENT TESTA GLABRA1* (*TTG1*), which encodes a WD-40 repeat protein. These proteins are able to form a MYB-bHLH-WD-repeat complex (Zhao et al. 2008), which activates the expression of *GLABRA*2 (*GL2*), a gene encoding a homeodomain transcription factor that promotes trichome initiation (Rerie et al. 1994). In addition to these positive regulatory genes, negative regulatory genes have also been identified, including *TRIPTYCHON* (*TRY*), *CAPRICE* (*CPC*), *ENHANCER OF TRY AND CPC 1* (*ETC1*), *ETC2*, *TRICHOMELESS1* (*TCL1*), *TCL2*, and *CPL3*, which encode R3 MYB transcription factors that compete with GL1 for binding to GL3/EGL3 to form an inactive complex (Ishida et al. 2008).

In contrast to *Arabidopsis* with its unicellular non-glandular trichomes, many asterid plants possess multicellular glandular trichomes (Yang et al. 2015). However, overexpression of *Arabidopsis GL1* in tobacco plants does not influence glandular trichome formation (Payne et al. 1999), suggesting that the molecular mechanism involved in controlling glandular trichome development may differ from that in *Arabidopsis*. Our current knowledge regarding this mechanism is limited; however, advances have been made with the discovery of some vital transcription factors (Chalvin et al. 2020). For instance, the R2R3 MYB transcription factor MIXTA has been found to positively regulate glandular trichome initiation in *Artemisia annua* (Shi et al. 2018) and tomato (*Solanum lycopersicum*) (Ewas et al. 2016). Another MYB protein in *A. annua*, AaMYB1, also promotes glandular trichome development (Matías-Hernández et al. 2017). In tomato (*S. lycopersicum*), the C2H2 zinc-finger gene *Hair* (Chang et al. 2018) and bHLH gene *SlMYC1* (Xu et al. 2018) have also been shown to positively regulate glandular trichome formation.

HD-ZIP IV transcription factors are also important regulators of glandular trichome development. For instance, AaHD1 and AaHD8 are two HD-ZIP IV proteins in *A. annua* that play important roles in glandular trichome development (Yan et al. 2017, 2018), while the AaHD8 homolog SlCD2 promotes glandular trichome initiation in tomato (*S. lycopersicum*) (Nadakuduti et al. 2012). *Woolly* (*Wo*) is another HD-ZIP IV transcription factor gene that controls glandular trichome formation in tomato (*S. lycopersicum*) (Yang et al. 2011). Microarray analysis has shown that *Wo* upregulates the expression of *SlCycB2*, a B-type cyclin gene, and direct protein–protein interactions are formed between Wo and SlCycB2 (Yang et al. 2011). Overexpression of *SlCycB2* results in significantly decreased numbers of both glandular and non-glandular trichomes. Meanwhile, RNA interference (RNAi) of *SlCycB2* leads to increased density of non-glandular type III and V trichomes and decreased density of glandular type I trichomes. However, glandular type IV and VI trichome density are not changed by RNAi of *SlCycB2* (Gao et al. 2017). These findings suggest that *SlCycB2* is a key regulatory gene in tomato trichome development, but also that it has different effects on the various types of trichomes. Specifically, *SlCycB2* negatively regulates non-glandular trichome formation, but has ambiguous effects on glandular trichomes.

In our previous study, we cloned the homologs of *Wo* and *SlCycB2* in *Nicotiana benthamiana* and found that *NbWo* and *NbCycB2* are able to control trichome development. Similar to that in tomato, *NbWo* could positively regulate trichome formation; however, unlike that in tomato, *NbCycB2* could negatively regulate glandular trichome formation. We further demonstrated that NbWo is able to directly bind the *NbCycB2* promoter and promote its expression. On the other hand, NbCycB2 represses the activity of NbWo through protein-protein interactions, thereby negatively regulating trichome formation (Wu et al. 2020).

Although the functions of *Wo* and *CycB2* in controlling glandular trichome initiation have been characterized and the relationships between them identified, this cannot explain the reason for *CycB2* having different effects on different types of trichomes, and thus, further information is still needed.

Taking this in consideration, we chose *Nicotiana tabacum* as a model system as it contains only three types of trichomes (Cui et al. 2011), being much simpler than tomato, which contains seven types (McDowell et al. 2011). We cloned *NtCycB2*, the homolog of *CycB2* in *N. tabacum*, and then constructed its overexpression (NtCycB2-OE) and knockout (NtCycB2-KO) lines. The effects of *NtCycB2* on trichome density and exudate content were analyzed by comparing the wild-type, overexpression, and knockout lines. We also conducted transcriptome analysis of NtCycB2-KO, NtCycB2-OE, and control plants to further explore the function of *NtCycB2*. Finally, the newly gained information and its implications for understanding the function of *NtCycB2* and the molecular mechanisms of multicellular glandular trichome formation were discussed.

Materials and methods

Plant materials and growth conditions

Tobacco (*Nicotiana tabacum*) cultivar K326 was used as the wild type, plants were grown under greenhouse conditions of 16 h light/8 h dark and 25 °C/20 °C day/night temperature.

Sequence analysis

The coding sequence (CDS) of *SlCycB2* (Gao et al. 2017) and *NbCycB2* (Wu et al. 2020) were used as queries to blast against the reference genome sequence of *N. tabacum* at Sol Genomics Network (SGN) database (https://solgenomics.net/), and e-value < $1e^{-10}$ was set as the query threshold. The CDS and amino acid sequence of the putative *NtCycB2* genes were downloaded; multiple sequence alignments were carried out using the Clustal Omega program (https://www.ebi.ac.uk/Tools/msa/clustalo/) using default parameters.

Vector construction and transformation of *N. tabacum*

The CRISPR/Cas9-mediated targeted mutagenesis was used to knockout *NtCycB2*, with the methods as described before (Gao et al. 2015), the targeting sequence (GTGATCAACCACCCACAAG) and its reverse complement oligomer were chemically synthesized and annealed, the dimers obtained were then inserted into the pORE-Cas9 binary vector (Gao et al. 2015). For *NtCycB2* overexpression, the full-length CDS were amplified (Primers are listed in Table S1) from the cDNA of *N. tabacum* leaves, and inserted into the pCXSN vector under the control of CaMV 35 S promoter (Chen et al. 2009).

The constructs obtained above were separately transformed into the competent cells of *Agrobacterium tumefaciens* strain GV3101 using the freeze-thaw method. Leaf discs from 6-week-old *N. tabacum* were infected by *A. tumefaciens* strain GV3101 harboring the *NtCycB2* knockout and overexpression vectors respectively using the methods described before (Gao et al. 2015). The leaf discs infected were then plated onto the regeneration medium (MS medium contains 3% (w/v) sucrose, 1 mg/L 6-Benzylaminopurine, 0.15 mg/L 1-Naphthaleneacetic acid and 50 mg/L Cefotaxime sodium, 8 mg/L hygromycin, pH 5.6). The hygromycin resistant seedlings were obtained, the genomic DNA was extracted using the DNeasy Plant Mini Kit (Qiagen, Germany) and used for further examination.

For the screening of *NtCycB2*-OE plants, PCR amplification of the hygromycin resistant gene from the genomic DNA was performed for preliminary screening (primers used were shown in Table S1), and the positive singletons were further confirmed by qRT-PCR measurement of *NtCycB2* expression level.

For the screening of NtCycB2-KO plants, the *NtCycB2* gene was amplified by PCR from genomic DNA (primers used were shown in Table S1), the PCR products were Sanger sequenced to detect the mutations.

Observation of trichome morphology

At the flowering stage, the newly emerged leaves (5 cm in length) of NtCycB2-KO, NtCycB2-OE, and control plants were collected and stained with 2% rhodamine B for 30 min, after washed away the unbound dye, the trichome was observed using a VHX-5000 microscope (Keyence, Japan). The trichome density was counted and shown as trichome number per mm^2 leaf area.

Analysis of trichome exudates

At the flowering stage, the trichome exudates of NtCycB2-KO, NtCycB2-OE and control plants were analyzed. Five healthy plants were selected from each line, and their middle leaves (10th to 12th leaf from the stem base) were collected. Leaf disks of 10 cm in diameter were cut out along both sides of the midrib, a total of 60 disks were obtained for each line, and divided into three repeats. Trichome exudates were extracted using the method described before (Huang et al. 2018). Briefly, leaf disks were immersed in 500 ml of dichloromethane for eight times of 2 s each. After that, 1 ml of internal standard solution (mixture of 2.020 mg/ml sucrose octaacetate and 2.542 mg/ml n-heptadecane alcohol) was added into each extract, well mixed and concentrated using a rotary evaporator, and finally dried in a nitrogen concentration. The extracts were then subjected to silylation treatment by adding 500 µl mixture of N,N-Dimethylformamide and N,O-Bis (trimethylsilyl) trifluoroacetamide (1:1, v:v), and incubated in 75 °C for 60 min.

The solutions obtained above were then analyzed by gas chromatography-mass spectrometry (GC-MS) using a TRACE GC ULTRA-DSQ II (Thermo Fisher Scientific, US) system coupled with a DB-5MS column (30 m × 0.25 mm) (Agilent Technologies, US). Helium was used as the carrier gas, the column flow was set as 0.8 ml/min. For each run, a volume of 1 µl sample was analyzed, with the split ratio set as 1:15. The injector temperature was 250 °C, and the oven was programmed to begin at 40 °C for 2 min, then 6 °C per min to 180 °C, hold for 2 min; the temperature then increased by 2 °C per min until it reached to 280 °C, and maintained at this temperature for 20 min. The MS transfer line temperature was 250 °C, and MS conditions were 50–650 AMU scanning range, and the ion source 230 °C. The MS profiles were used to identify components based

on the NIST12 spectral library (https://www.nist.gov/srd). For each component, the area under the corresponding GC chromatogram peak was integrated, and compared to that of the internal standard, so that their amounts were calculated.

Aphid bioassay

Tobacco aphids (*Myzus nicotianae*) resistance of NtCycB2-KO, NtCycB2-OE, and control plants were compared at the 8-leaf stage. Four healthy plants for each line were selected, and ten aphid larvae were inoculated on the leaves for each plant. Each plant was confined to a cage assembled with an insect proof net, and grown in a chamber with conditions of 25 °C, 70% relative humidity, and 16:8 h light/dark photoperiod. The aphid number was calculated every week for a nine-week period.

RNA extraction

Different plant tissues were harvested and frozen immediately using liquid nitrogen. Total RNA was isolated using TRIzol reagent (Invitrogen, US). The integrity of the RNA samples was examined by 1% agarose gel electrophoresis. The quality and quantity of these RNA samples were further determined by measuring the relative absorbance at 260/280 and 260/230 nm using NanoDrop 2000 spectrophotometer (Thermo Fisher Scientific, US).

RNA-Seq analysis

The RNA-Seq libraries were produced and sequenced in Shanghai OE Biotech Co., Ltd (China) using the Illumina HiSeq^{TM} 2000 sequencing platform. 150 bp paired-end clean reads were generated from the raw data by removing the adaptors and low-quality reads. All the clean reads were then mapped to the *N. tabacum* reference genome (ftp://ftp.solgenomics.net/genomes/Nicotiana_tabacum/edwards_et_al_2017/assembly/Nitab-v4.5_genome_Scf_Edwards2017.fasta) (Edwards et al. 2017) using hisat2 software (Kim et al. 2015). Gene expression levels were calculated as FPKM, and differentially expressed genes (DEGs) were identified using the DESeq R package (Anders and Huber 2012), P-value < 0.05, fold change < 0.5 or > 2 were set as the thresholds for significantly differential expression. To analysis the function of DEGs, Gene Ontology (GO) functional enrichment analysis was performed using topGO (Alexa and Rahnenfuhrer 2010) software.

Quantitative real time PCR (qRT-PCR)

First-strand cDNA was synthesized from 2 µg of total RNA using Goscritp reverse transcriptase (Promega, US). qRT-PCR reaction mixture contains 10 µl of SYBR Green I Master Mix (TOYOBO, Japan), 0.5 µl of forward primers (10 µM), 0.5 µl of reverse primers (10 µM), 1 µl of cDNA template and 8 µl of distilled water. qRT-PCR was performed on the Roche Light Cycler 480 system (Roche, Switzerland) with the parameters set as follows: 95 °C for 2 min, followed by 40 cycles of 95 °C for 15 s, annealing temperature for 30 s, and 72 °C for 20 s. A melting curve was established by slow heating from 60 to 95 °C within 20 min. Relative gene expression levels were calculated using $2^{-\Delta\Delta Ct}$, with three technical replicates for each sample and the results were shown as means ± standard deviation (SD). All the primers used are listed in Table S1.

Statistical analysis

For the experiments described above, three separate tests were carried out for each sample. The data obtained were subjected to one-way analysis of variance (ANOVA) using IBM SPSS Statistics 19 software (IBM, New York, USA), followed by the least significant difference multiple comparison test. Statistical significance of the difference between data obtained from different materials was considered at $P < 0.05$.

Results

NtCycB2 negatively regulated tobacco long stalk glandular trichome (LGT) initiation

Two loci, *Nitab4.5_0014697g0010.1* and *Nitab4.5_0012062g0010.1*, were identified as putative homologs of *CycB2* in the *N. tabacum* reference genome (Edwards et al. 2017) and were arbitrarily designated as *NtCycB2-1* and *NtCycB2-2*, respectively. Both contained a 333-bp open reading frame (Fig. S1a), and no introns were found in their genomic sequence. Their protein sequences were identical to each other (Fig. S1b) and showed 96.4% and 71.1% identity to NbCycB2 and SlCycB2 protein sequences, respectively.

The expression pattern of *NtCycB2* was examined in different plant tissues, including roots, stems, leaves, flowers, and trichomes separated from leaves. *NtCycB2* showed the highest expression in trichomes and the lowest in roots, while its expression in flowers was higher than that in leaves and stems. When comparing *NtCycB2-1* and *NtCycB2-2*, we found that *NtCycB2-1* was expressed at higher levels than that of *NtCycB2-2* in all tissues except the roots (Fig. S1c).

We then constructed the *NtCycB2* knockout line NtCycB2-KO using a CRISPR-Cas9 system. Sanger sequencing showed that a 7-bp deletion was induced for *NtCycB2-1*, and a 5-bp deletion coupled with an A/T bp insertion was found for *NtCycB2-2* (Fig. 1a). The

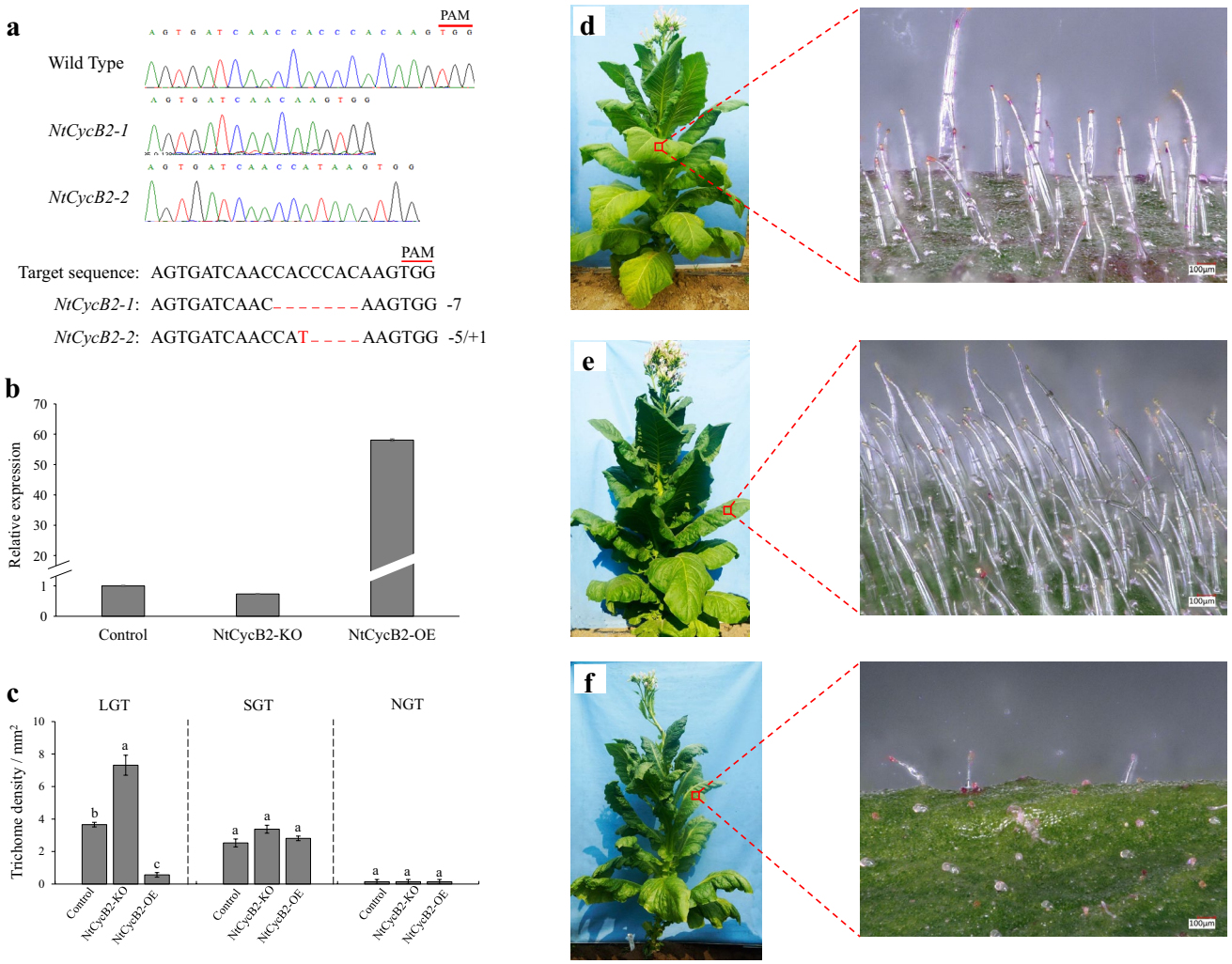

Fig. 1 Construction of *NtCycB2* knockout and overexpression lines and observation of leaf trichome. **a** Targeted mutagenesis of *NtCycB2* gene using CRISPR-Cas9 system. DNA insertions and deletions are shown in red letters and dashes. PAM, the protospacer adjacent motif. **b** Relative expression of *NtCycB2* in NtCycB2-KO, NtCycB2-OE and control plants measured by qRT-PCR, the columns and bars represent the means and standard errors (n = 3) respectively. The relative expression levels in different plants were calculated by setting the expression value in control plants as 1. **c** Statistics of the leaf trichome density. Representative phenotype pictures for **d** wild type, **e** NtCycB2-KO and **f** NtCycB2-OE are shown here

NtCycB2-1 coding sequence was used to construct the overexpression line NtCycB2-OE. A pair of conserved primers (Table S1) was designed to estimate the total *NtCycB2-1* and *NtCycB2-2* expression. Based on qRT-PCR analysis, there was a 58-fold higher expression level of *NtCycB2* in NtCycB2-OE than that in control plants (Fig. 1b). Three types of trichomes, long stalk glandular trichomes (LGT), short stalk glandular trichomes (SGT), and non-glandular trichomes (NGT) were found on the leaf surface of wild-type plants (Fig. 1d). Compared to that of the control plants, significantly more trichomes were observed on the leaves and stems of NtCycB2-KO plants (Fig. 1e). In contrast, a hairless phenotype was observed in NtCycB2-OE plants (Fig. 1f). The densities of LGT, SGT, and NGT were individually calculated to elucidate detailed changes. The results showed that LGT density in NtCycB2-KO plants was two-fold higher than that of the control plants, whereas in NtCycB2-OE plants was 15% of that in control plants. However, no significant changes were found for SGT and NGT densities in either NtCycB2-KO or NtCycB2-OE plants compared to those of the control plants (Fig. 1c). We also examined the flower phenotypes, since *NtCycB2* showed a higher expression in flowers than that in leaves, as shown in Fig. S2, flowers of both NtCycB2-KO and NtCycB2-OE plants were well developed. LGT density was increased in NtCycB2-KO flowers but decreased in NtCycB2-OE flowers, which is similar to that in leaves. These results suggest that

NtCycB2 negatively regulated the formation of LGT, but had no effect on that of SGT or NGT.

NtCycB2 affected the accumulation of leaf surface chemical components

We analyzed the trichome exudates of NtCycB2-KO, NtCycB2-OE, and control plants. The main components of tobacco glandular trichomes are generally diterpenoids and sugar esters (Huang et al. 2018). GC-MS analysis showed that the quantity of both diterpenoids and sugar esters in NtCycB2-KO plants was significantly increased, specifically 1.76-fold for diterpenoids and 1.36-fold for sugar esters, compared to that in control plants (Fig. 2b, c). Conversely, the quantity of diterpenoids and sugar esters in NtCycB2-OE plants was dramatically decreased to only 7.1% for diterpenoids and 24.4% for sugar esters relative to that in wild-type plants (Fig. 2b, c).

NtCycB2 affected tobacco resistance to aphids

We investigated aphid resistance differences between NtCycB2-KO, NtCycB2-OE, and control plants by comparing aphid survival and reproduction. Ten aphids were transferred to each tobacco plant, and the aphid number was determined weekly. Our results showed that the aphid number for NtCycB2-OE plants was much higher than that for control plants throughout the experimental period (Fig. 3b, d). In contrast, NtCycB2-KO plants showed fewer aphids than that of the control plants (Fig. 3c, d). The aphid number reached its highest point five weeks after the initial infestation, and the average aphid number for NtCycB2-OE plants was 3.5-fold higher than that for control plants. In contrast, the aphid number for the NtCycB2-KO plants was reduced to only 25% of that for wild-type plants (Fig. 3d). These results suggest that aphid resistance was increased in NtCycB2-KO plants and decreased in NtCycB2-OE plants.

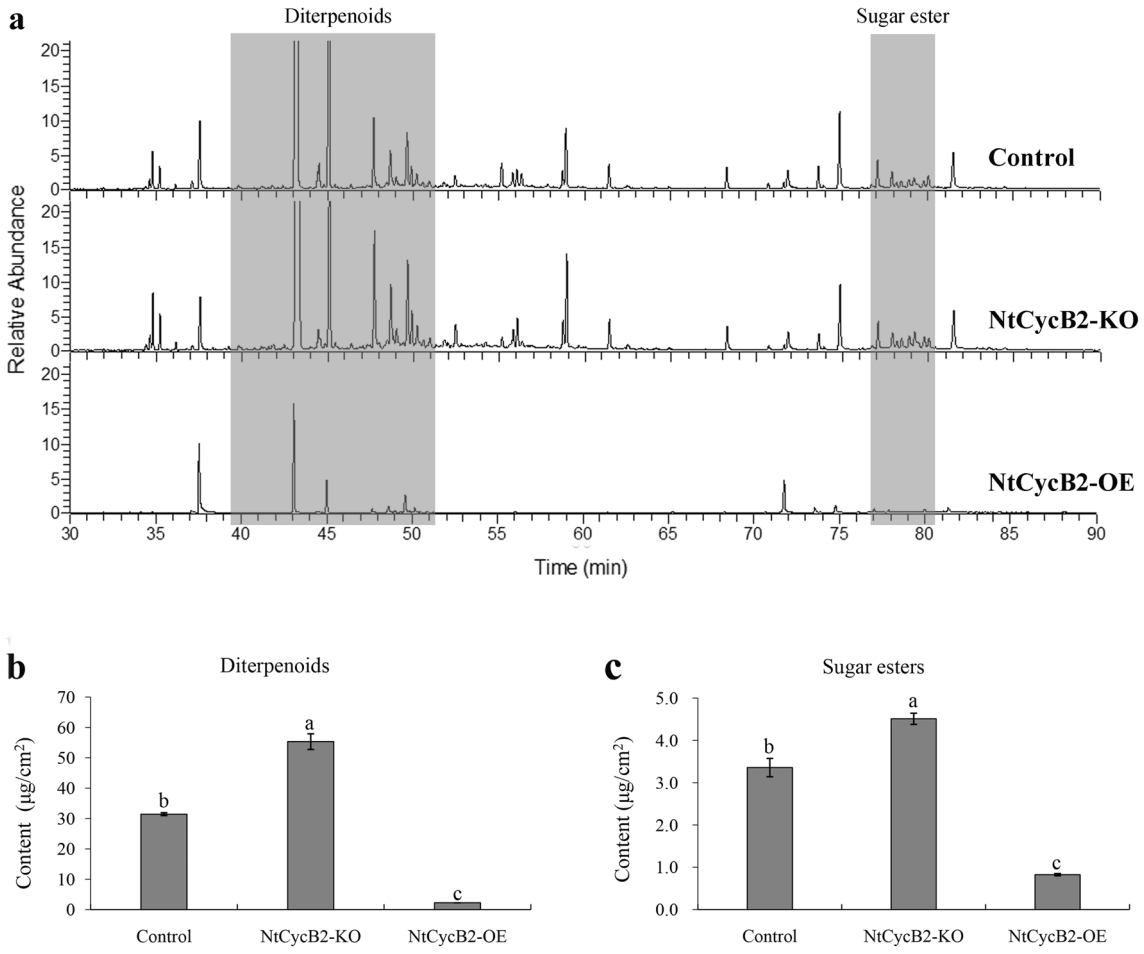

Fig. 2 GC-MS analysis of glandular trichome exudates. **a** GC-MS profiles of trichome exudates on control, NtCycB2-KO and NtCycB2-OE plants. **b** Statistics of diterpenoids content. **c** Statistics of sugar ester content. The columns and bars represent the means and standard errors (n = 3) respectively. The means marked by different letters are statistically significant ($P < 0.05$)

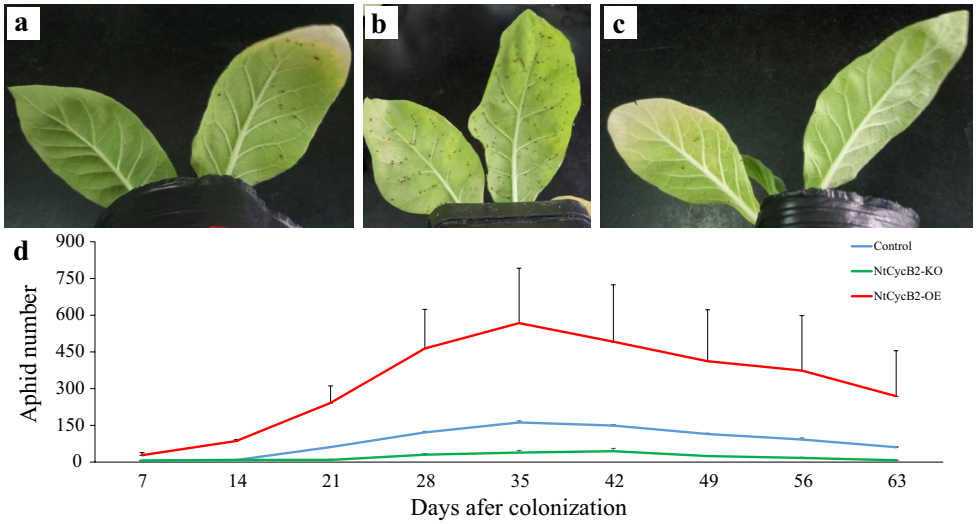

Fig. 3 Aphid resistance analysis. Phenotype of aphid resistance for **a** control, **b** NtCycB2-OE and **c** NtCycB2-KO. **d** Statistics of aphid number. Photos shown in panel A–C were taken 35 days after colonization

NtCycB2 manipulation triggered gene expression profile changes

We performed a comparative transcriptome analysis of NtCycB2-KO, NtCycB2-OE, and control plants. Three independent biological replicates were used for each line. Approximately 47 million paired-end clean reads of 150 bp in length were generated for each sample. Approximately 97% of the clean reads were successfully mapped to the *N. tabacum* reference genome (Edwards et al. 2017), and approximately 87% of the reads were uniquely mapped (Table S2). Sample cluster analysis based on gene expression showed that the biological replicates were more highly correlated within samples than between samples (Fig. S3a). These results suggest that the quality of the sequence data was sufficient for subsequent gene expression analysis.

Gene expression levels were compared between different samples, and differentially expressed genes (DEGs) were defined as fold change < 0.5 or > 2. Statistical significance was set at P-value < 0.05. Compared with that of the control plants, 1,235 DEGs were upregulated and 1,317 DEGs were downregulated in NtCycB2-KO plants, while 1,063 DEGs were upregulated and 870 DEGs were downregulated in NtCycB2-OE plants. To further confirm the RNA-Seq results, 17 DEGs were randomly selected, and their expression were validated using qRT-PCR (genes and primers are listed in Table S1). The results showed that gene expression levels measured by qRT-PCR and RNA-Seq had a strong correlation (R^2 = 0.71) (Fig. S3b), indicating the high quality of our RNA-Seq results.

Among the 2,552 total DEGs in NtCycB2-KO plants and 1,933 total DEGs in NtCycB2-OE plants, 695 were shared by both plant lines (Fig. 4a). We performed Gene Ontology (GO) enrichment of these common DEGs to evaluate their functional categories. The GO terms of the enriched biological processes are listed in Table S5. The top 20 most significant GO terms are shown in Fig. 4b and are mainly involved in ion transport, carbohydrate and amino acid metabolism, photosynthesis, and transcription regulation processes.

We speculated that the DEGs showing opposite changes in NtCycB2-KO and NtCycB2-OE plants were functionally associated with *NtCycB2*. As shown in the Venn diagram (Fig. 4c), 25 DEGs were upregulated in NtCycB2-KO plants and downregulated in NtCycB2-OE plants, while only 13 DEGs were downregulated in NtCycB2-KO plants and upregulated in NtCycB2-OE plants (Fig. 4d), and they were listed in Table S6. Among the group of 25 DEGs in Fig. 4c and 13 were related to secondary metabolite biosynthesis and transport, while five were related to abiotic or biotic stress resistance (Fig. 4e, Table S6). Among the group of 13 DEGs in Fig. 4d, three were related to secondary metabolite biosynthesis and four were related to abiotic or biotic stress resistance (Fig. 4f, Table S6). These results indicated that in addition to trichome formation, *NtCycB2* may also regulate metabolic processes and environmental stress resistance.

Interestingly, among the group of 25 DEGs in Fig. 4c, two transcription factor genes were identified, namely *Nitab4.5_0004186g0020.1* and *Nitab4.5_0005769g0080.1*, both belonging to the MYB family. Expression of *Nitab4.5_0004186g0020.1* and *Nitab4.5_0005769g0080.1* was confirmed using qRT-PCR (Fig. S4), indicating that they may work in conjunction with *NtCycB2* to control the formation of glandular trichomes.

NtCycB2 affected the expression of diterpenoid biosynthesis-related genes

Changes in the amounts of trichome exudate and the DEGs related to secondary metabolite biosynthesis prompted us

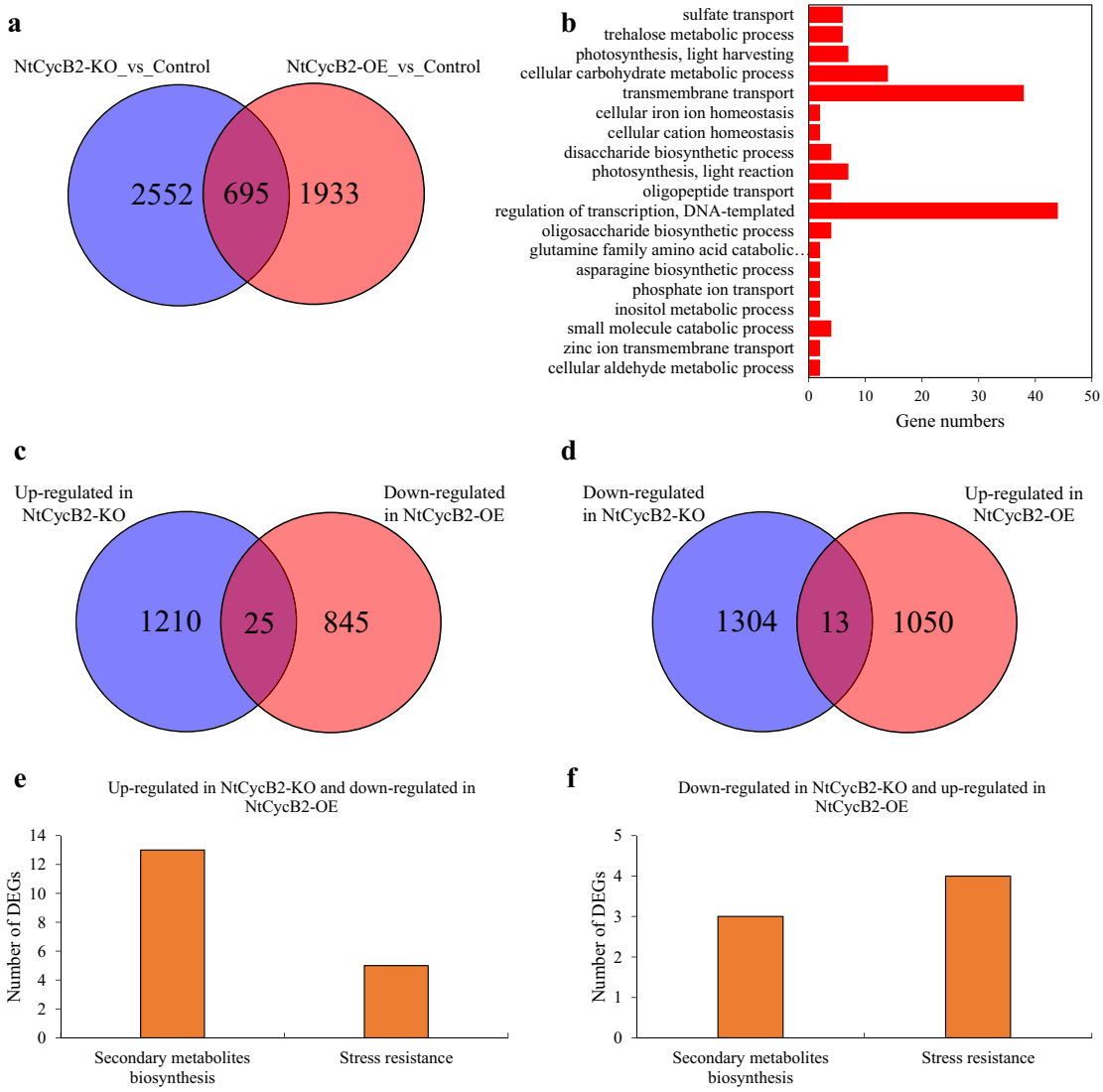

Fig. 4 RNA-Seq analysis of control, NtCycB2-KO and NtCycB2-OE plants. **a** Venn diagram showing common and exclusive DEGs between NtCycB2-KO and NtCycB2-OE. **b** Top 20 most significant enriched GO terms of the common 695 DEGs between NtCycB2-KO and NtCycB2-OE. **c** Venn diagram showing common and exclusive DEGs that up regulated in NtCycB2-KO and down regulated in NtCycB2-OE. **d** Venn diagram showing common and exclusive DEGs that down regulated in NtCycB2-KO and up regulated in NtCycB2-OE. **e** Gene numbers of secondary metabolites biosynthesis and resistance response among the 25 DEGs that up regulated in NtCycB2-KO and down regulated in NtCycB2-OE. **f** Gene numbers of secondary metabolites biosynthesis and resistance response among the 13 DEGs that down regulated in NtCycB2-KO and up regulated in NtCycB2-OE

to compare the expression levels of diterpenoid biosynthesis genes. In tobacco glandular trichomes, diterpenoid biosynthesis is catalyzed by four enzymes, cembratrien-ol synthases (CBTS), cytochrome P450 (CYP71D16), copalyl diphosphate synthases (CPS2), and abienol synthase (ABS) (Wang and Wagner 2003; Sallaud et al. 2012). Based on the fragments per kilobase of transcript per million mapped reads (FPKM) values of these four gene families, we found that most of them were upregulated in NtCycB2-KO plants, but downregulated in NtCycB2-OE plants (Fig. 5). To further confirm these results, one member from each gene family was randomly selected, and their expression analyzed using qRT-PCR. Although some quantitative differences existed at the expression level, the qRT-PCR results revealed similar expression patterns to those of the RNA-Seq data (Fig. S4).

Homologs of known trichome development-related genes were not regulated by *NtCycB2*

Many trichome development regulatory genes have been identified, such as *GL1*, *GL3/EGL3*, and *TTG1* in

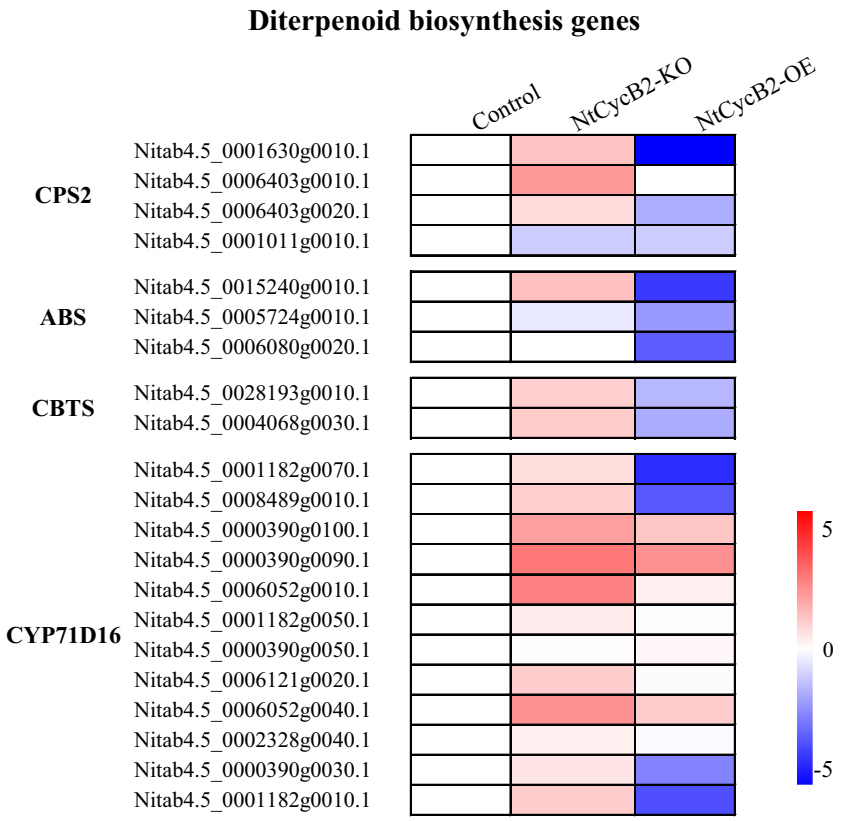

Fig. 5 Heat map of gene expression difference in diterpenoids biosynthesis pathway between control, NtCycB2-KO and NtCycB2-OE plants. Log_2foldchanges were shown here. *CPS2* copalyl diphosphate synthases, *ABS* abienol synthase, *CBTS* cembratrien-ol synthases, *CYP71D16* cytochrome P450

Arabidopsis (Pattanaik et al. 2014), *Wo* and *SlCycB2* in tomato (Yang et al. 2011; Gao et al. 2017), and *AaMIXTA* and *AaHD1* in *A. annua* (Yan et al. 2017; Shi et al. 2018). We compared the expression levels of tobacco homologs of 23 known trichome development-related genes (Table S7). Although the expression of some genes changed, these expression changes were only significant for a small number of genes, and changes in expression were not consistent with changes in trichome density. This suggested that these genes may not be associated with *NtCycB2*.

Discussion

Trichomes, especially glandular trichomes, can protect plants from damage by various biotic and abiotic stressors (Glas et al. 2012), thus increasing trichome density is an efficient way to improve plant resistance. Therefore, a deep study of the molecular mechanisms controlling multicellular glandular trichome formation will aid in increasing trichome density. *CycB2* encodes a putative B-type cyclin and is a key gene regulating trichome initiation in tomato and *N. benthamiana* (Gao et al. 2017; Wu et al. 2020), but the detailed mechanism remains unclear.

In this study, we cloned *NtCycB2*, the homolog of *CycB2* in *N. tabacum*. We then analyzed the role of *NtCycB2* in the formation of different types of trichomes, biosynthesis of trichome exudates, and aphid resistance by generating overexpression and knockout tobacco lines. Furthermore, we identified genes through RNA-Seq analysis that may be regulated by *NtCycB2*. Our results provide new information regarding the function of *NtCycB2*.

NtCycB2 has different roles in glandular and non-glandular trichome formation

Previous studies have shown that suppression of *CycB2* increases trichome density in both tomato and *N. benthamiana*, while overexpression of *CycB2* causes a hairless phenotype (Gao et al. 2017; Wu et al. 2020). We obtained similar results in our study, but differences still exist in these similar appearances. In tomato plants, which are covered by seven types of trichomes (Glas et al. 2012), the non-glandular trichome (type III and V) numbers are dramatically decreased in *SlCycB2* overexpression plants, but significantly increased in *SlCycB2* RNAi lines, suggesting that non-glandular trichomes formation is negatively regulated by *SlCycB2*. Regarding glandular trichomes (type I, IV, VI, and VII), type I are almost absent in both *SlCycB2* overexpression and RNAi plants, whereas type IV and VI glandular trichome density is decreased in *SlCycB2* overexpression lines but not changed in *SlCycB2* RNAi plants (Gao et al. 2017). This makes it difficult to define the role of *SlCycB2* in glandular trichome formation. In contrast,

CycB2 in *N. benthamiana* has been shown to be a negative regulator of glandular trichomes, as their density decreases in *NbCycB2* overexpression lines and increases in *NbCycB2* RNAi lines (Wu et al. 2020). However, *N. benthamiana* does not possess non-glandular trichomes and thus, it was not clear whether *CycB2* has any effects on non-glandular trichomes in tobacco plants. In our study, *NtCycB2* negatively regulated LGT formation but had no effect on SGT or NGT formation (Fig. 1). These inconsistent results indicate that *CycB2* has different roles in the formation of glandular and non-glandular trichomes and that the function of *CycB2* in trichome formation may differ among Solanaceae species.

Previous studies have also found that the function of some trichome regulatory genes is conserved among different species, such as MIXTA in *A. annua* (Shi et al. 2018) and tomato plants (Ewas et al. 2016), and AaHD8 in *A. annua* (Yan et al. 2018) and its homolog SlCD2 in tomato plants (Nadakuduti et al. 2012). However, few studies have compared their roles in different trichome types among species. Here, we found that even though *CycB2* decreased trichome density in tomato plants, *N. benthamiana*, and *N. tabacum*, it had different impacts on glandular and non-glandular trichomes. This finding expands our knowledge about multicellular trichome formation.

NtCycB2 negatively regulates the accumulation of leaf surface chemical components and aphid resistance

Trichomes play an important role in response to biotic stress, as they not only act as a physical barrier against herbivores, but, due to their exudates, also provide chemical protection (Huchelmann et al. 2017; Alain 2018). Consistent with this, our study showed that knocking out of *NtCycB2* significantly increased aphid resistance (Fig. 3). Based on our results, we speculate that *NtCycB2* regulated tobacco aphid resistance in three ways.

First, *NtCycB2* was able to dramatically influence trichome density, which directly enhanced the physical barrier. Furthermore, more glandular trichomes meant more "factories" for the biosynthesis of exudates, which further strengthened aphid resistance.

Second, *NtCycB2* negatively regulated the expression of trichome exudate biosynthesis genes, as they were upregulated in NtCycB2-KO plants and downregulated in NtCycB2-OE plants (Fig. 5). Consistent with this, *NtCycB2* showed a higher expression level in trichomes than that in other tissues we examined (Fig. S1c). Thus, changes in the accumulation of leaf surface chemical components may have been partially due to changes in the expression of these genes. It has also been found in previous studies that some trichome formation-related transcription factors have a dual function. In addition to controlling trichome initiation, these transcription factors are able to regulate trichome metabolism. For example, the AP2 transcription factor TAR1 of *A. annua* regulates the development of trichomes and biosynthesis of artemisinin (Tan et al. 2015), and the transcription factor SlMYC1 of tomato plants regulates type VI glandular trichome formation and terpenoid biosynthesis (Xu et al. 2018). A recent study showed that SlWo in tomato plants can directly bind the promoter of terpene synthase genes and activate their expression (Hua et al. 2021), indicating that the CycB2-Wo pathway (Wu et al. 2020) may also participate in tobacco trichome secondary metabolite biosynthesis.

Third, *NtCycB2* regulated the expression of other resistance-related genes. Among the DEGs that exhibited opposite changes in NtCycB2-KO and NtCycB2-OE plants, many were involved in abiotic/biotic stress resistance (Table S6), which provided additional protection against aphid invasion. Similar to our results, *SlCycB2* in tomato plants regulates the expression of defense-related genes, such as protein inhibitors (Gao et al. 2017).

NtCycB2 may regulate trichome formation through pathways that different from those of known genes

NbCycB2 has been found to influence trichome formation through the CycB2-Wo feedback loop by suppressing the activity of the NbWo protein in *N. benthamiana* (Wu et al. 2020). However, it is unknown whether other genes are involved in this process. Therefore, further investigation is needed.

Trichome formation regulating genes have been identified in many species, such as *Arabidopsis* (Pattanaik et al. 2014), cotton (Yang and Ye 2013), *A. annua*, and tomato (Chalvin et al. 2020), and previous studies suggest that their function may be conserved in different plant species (Payne et al. 1999; Chang et al. 2018). We identified the homologs of 23 known trichome-related genes in tobacco (Table S7), and their expression in NtCycB2-KO, NtCycB2-OE, and control plants were compare using RNA-Seq data. However, none showed an expression pattern related with the changes in glandular trichome density. Similarly, in a previous study, the expression of known trichome-related genes showed no significant changes when tomato *Wo* was ectopically expressed in *N. tabacum* (Yang et al. 2015). This indicates that the expression of these genes is not regulated by *NtCycB2* and that they may not participate in *NtCycB2*-regulated trichome formation pathways.

Interestingly, two transcription factor genes were identified among the DEGs that were upregulated in NtCycB2-KO plants and downregulated in NtCycB2-OE plants, *Nitab4.5_0004186g0020.1* and *Nitab4.5_0005769g0080.1* (Table S6).

Nitab4.5_0004186g0020.1 is a RADIALIS-like protein, which is a member of MYB transcription factor family. A previous study showed that the *RADIALIS*-like gene *GbRL1* of cotton is strongly expressed in ovules and cotton fiber during the initiation stage. The authors of that study inferred that *GbRL1* may play a role in fiber initiation (Zhang et al. 2011), which is a process similar to trichome formation. Meanwhile, Nitab4.5_0005769g0080.1 is a homolog of the *Arabidopsis* MYB108 protein. In *Arabidopsis*, MYB108 is a jasmonic acid (JA)-inducible transcription factor that plays an important role in stamen development (Mandaokar and Browse 2009) and biotic stress responses (Mengiste et al. 2003). In many plant species, it has been found that JA plays an important role in trichome development (Boughton et al. 2005; Qi et al. 2011; Yan et al. 2017), suggesting that this gene may also regulate glandular trichome development in tobacco. We hypothesize that these two transcription factors may regulate tobacco glandular trichome development, but this requires further study.

Supplementary Information The online version contains supplementary material available at https://doi.org/10.1007/s11103-021-01222-z.

Acknowledgements We thank Professor Liang Chen (Xiamen University) for helping with vector construction.

Author Contributions All authors contributed to the study conception and design. HC and ZW designed the study. ZW, XY, YM, and YP performed the experiments. ZW, HZ and HC analyzed the data, ZW and H. C. wrote the manuscript.

Funding This research was financially supported by the National Science Foundation of Henan province (Grant No. 182300410094), the State Tobacco Monopoly Administration of China [Grant No. 110202101005 (JY-05)], and China Tobacco Henan Industrial Co., Ltd. [Grant No. AW202149].

Data Availability All data generated or analyzed during this study are included in this published article (and its supplementary information files). The raw filtered RNA-seq data used in this article are available in the NCBI Sequence Read Archive (SRA) (https://www.ncbi.nlm.nih.gov/sra/) under BioProject Accession: PRJNA622901.

Declarations

Conflict of interest The authors declare that there are no conflicts of interest.

References

Alain T (2018) Harnessing plant trichome biochemistry for the production of useful compounds. In: Kermode AR, Jiang L (eds) Molecular pharming: applications, challenges, and emerging areas. Wiley, Hoboken, pp 353–382

Alexa A, Rahnenfuhrer J (2010) topGO: enrichment analysis for gene ontology. Bioconductor R package. http://www.bioconductor.org/packages/2.6/bioc/vignettes/topGO/inst/doc/topGO.pdf. Accessed 4 June 2010.

Anders S, Huber W (2012) Differential expression of RNA-Seq data at the gene level–the DESeq package. Eur Mol Biol Lab. https://www.genomatix.de/online_help/help_regionminer/DESeq_1.10.1.pdf. Accessed 12 Sept 2012.

Boughton AJ, Hoover K, Felton GW (2005) Methyl jasmonate application induces increased densities of glandular trichomes on tomato, *Lycopersicon esculentum*. J Chem Ecol 31(9):2211–2216. https://doi.org/10.1007/s10886-005-6228-7

Chalvin C, Drevensek S, Dron M, Bendahmane A, Boualem A (2020) Genetic control of glandular trichome development. Trends Plant Sci 25(5):477–487. https://doi.org/10.1016/j.tplants.2019.12.025

Chang J, Yu T, Yang Q, Li C, Xiong C, Gao S, Xie Q, Zheng F, Li H, Tian Z, Yang C, Ye Z (2018) *Hair*, encoding a single C2H2 zinc-finger protein, regulates multicellular trichome formation in tomato. Plant J 96(1):90–102. https://doi.org/10.1111/tpj.14018

Chen S, Songkumarn P, Liu J, Wang G-L (2009) A versatile zero background T-vector system for gene cloning and functional genomics. Plant Physiol 150(3):1111–1121. https://doi.org/10.1104/pp.109.137125

Cui H, Zhang S-T, Yang H-J, Ji H, Wang X-J (2011) Gene expression profile analysis of tobacco leaf trichomes. BMC Plant Biol 11(1):76. https://doi.org/10.1186/1471-2229-11-76

Edwards KD, Fernandez-Pozo N, Drake-Stowe K, Humphry M, Evans AD, Bombarely A, Allen F, Hurst R, White B, Kernodle SP, Bromley JR, Sanchez-Tamburrino JP, Lewis RS, Mueller LA (2017) A reference genome for *Nicotiana tabacum* enables map-based cloning of homeologous loci implicated in nitrogen utilization efficiency. BMC Genom 18:448. https://doi.org/10.1186/s12864-017-3791-6

Ewas M, Gao Y, Wang S, Liu X, Zhang H, Nishawy EME, Ali F, Shahzad R, Ziaf K, Subthain H, Martin C, Luo J (2016) Manipulation of SlMXl for enhanced carotenoids accumulation and drought resistance in tomato. Sci Bull 61(18):1413–1418. https://doi.org/10.1007/s11434-016-1108-9

Gao J, Wang G, Ma S, Xie X, Wu X, Zhang X, Wu Y, Zhao P, Xia Q (2015) CRISPR/Cas9-mediated targeted mutagenesis in *Nicotiana tabacum*. Plant Mol Biol 87(1):99–110. https://doi.org/10.1007/s11103-014-0263-0

Gao S, Gao Y, Xiong C, Yu G, Chang J, Yang Q, Yang C, Ye Z (2017) The tomato B-type cyclin gene, *SlCycB2*, plays key roles in reproductive organ development, trichome initiation, terpenoids biosynthesis and *Prodenia litura* defense. Plant Sci 262:103–114. https://doi.org/10.1016/j.plantsci.2017.05.006

Glas J, Schimmel B, Alba J, Escobar-Bravo R, Schuurink R, Kant M (2012) Plant glandular trichomes as targets for breeding or engineering of resistance to herbivores. Int J Mol Sci 13(12):17077–17103. https://doi.org/10.3390/ijms131217077

Hua B, Chang J, Wu M, Xu Z, Zhang F, Yang M, Xu H, Wang L-J, Chen X-Y, Wu S (2021) Mediation of JA signalling in glandular trichomes by the *woolly/SlMYC1* regulatory module improves pest resistance in tomato. Plant Biotechnol J 19(2):375–393. https://doi.org/10.1111/pbi.13473

Huang M, Zhang H, Wang Z, Niu D, Li Y, Cui H (2018) Comparative studies of leaf surface chemical biosynthesis in different tobacco cultivars. Acta Physiol Plant 40(4):67. https://doi.org/10.1007/s11738-018-2642-7

Huchelmann A, Boutry M, Hachez C (2017) Plant glandular trichomes: natural cell factories of high biotechnological interest. Plant Physiol 175(1):6–22. https://doi.org/10.1104/pp.17.00727

Ishida T, Kurata T, Okada K, Wada T (2008) A genetic regulatory network in the development of trichomes and root hairs. Annu Rev Plant Biol 59(1):365–386. https://doi.org/10.1146/annurev.arplant.59.032607.092949

Karabourniotis G, Kotsabassidis D, Manetas Y (1995) Trichome density and its protective potential against ultraviolet-B radiation damage during leaf development. Can J Bot 73(3):376–383. https://doi.org/10.1139/b95-039

Karabourniotis G, Liakopoulos G, Nikolopoulos D, Bresta P (2019) Protective and defensive roles of non-glandular trichomes against multiple stresses: structure–function coordination. J For Res 31(1):1–12. https://doi.org/10.1007/s11676-019-01034-4

Kim D, Langmead B, Salzberg SL (2015) HISAT: a fast spliced aligner with low memory requirements. Nat Methods 12(4):357–360. https://doi.org/10.1038/NMETH.3317

Mandaokar A, Browse J (2009) MYB108 acts together with MYB24 to regulate jasmonate-mediated stamen maturation in *Arabidopsis*. Plant Physiol 149(2):851–862. https://doi.org/10.1104/pp.108.132597

Matías-Hernández L, Jiang W, Yang K, Tang K, Brodelius PE, Pelaz S (2017) AaMYB1 and its orthologue AtMYB61 affect terpene metabolism and trichome development in *Artemisia annua* and *Arabidopsis thaliana*. Plant J 90(3):520–534. https://doi.org/10.1111/tpj.13509

McDowell ET, Kapteyn J, Schmidt A, Li C, Kang JH, Descour A, Shi F, Larson M, Schilmiller A, An L, Jones AD, Pichersky E, Soderlund CA, Gang DR (2011) Comparative functional genomic analysis of *Solanum* glandular trichome types. Plant Physiol 155(1):524–539. https://doi.org/10.1104/pp.110.167114

Mengiste T, Chen X, Salmeron J, Dietrich R (2003) The *BOTRYTIS SUSCEPTIBLE1* gene encodes an R2R3MYB transcription factor protein that is required for biotic and abiotic stress responses in *Arabidopsis*. Plant Cell 15(11):2551–2565. https://doi.org/10.1105/tpc.014167

Nadakuduti SS, Pollard M, Kosma DK, Allen C, Ohlrogge JB, Barry CS (2012) Pleiotropic phenotypes of the *sticky peel* mutant provide new insight into the role of *CUTIN DEFICIENT2* in epidermal cell function in tomato. Plant Physiol 159(3):945–960. https://doi.org/10.1104/pp.112.198374

Pattanaik S, Patra B, Singh SK, Yuan L (2014) An overview of the gene regulatory network controlling trichome development in the model plant, *Arabidopsis*. Front Plant Sci 5:259. https://doi.org/10.3389/fpls.2014.00259

Payne T, Clement J, Arnold D, Lloyd A (1999) Heterologous myb genes distinct from *GL1* enhance trichome production when overexpressed in *Nicotiana tabacum*. Development 126(4):671–682. https://doi.org/10.1242/dev.126.4.671

Qi T, Song S, Ren Q, Wu D, Huang H, Chen Y, Fan M, Peng W, Ren C, Xie D (2011) The jasmonate-ZIM-domain proteins interact with the WD-Repeat/bHLH/MYB complexes to regulate jasmonate-mediated anthocyanin accumulation and trichome initiation in *Arabidopsis thaliana*. Plant Cell 23(5):1795–1814. https://doi.org/10.1105/tpc.111.083261

Rerie WG, Feldmann KA, Marks MD (1994) The *GLABRA2* gene encodes a homeo domain protein required for normal trichome development in *Arabidopsis*. Gene Dev 8(12):1388–1399. https://doi.org/10.1101/gad.8.12.1388

Sallaud C, Giacalone C, Topfer R, Goepfert S, Bakaher N, Rosti S, Tissier A (2012) Characterization of two genes for the biosynthesis of the labdane diterpene Z-abienol in tobacco (*Nicotiana tabacum*) glandular trichomes. Plant J 72(1):1–17. https://doi.org/10.1111/j.1365-313X.2012.05068.x

Shi P, Fu X, Shen Q, Liu M, Pan Q, Tang Y, Jiang W, Lv Z, Yan T, Ma Y, Chen M, Hao X, Liu P, Li L, Sun X, Tang K (2018) The roles of *AaMIXTA1* in regulating the initiation of glandular trichomes and cuticle biosynthesis in *Artemisia annua*. New Phytol 217(1):261–276. https://doi.org/10.1111/nph.14789

Tan H, Xiao L, Gao S, Li Q, Chen J, Xiao Y, Ji Q, Chen R, Chen W, Zhang L (2015) *TRICHOME AND ARTEMISININ REGULATOR 1* is required for trichome development and artemisinin biosynthesis in *Artemisia annua*. Mol Plant 8(9):1396–1411. https://doi.org/10.1016/j.molp.2015.04.002

Wang E, Wagner GJ (2003) Elucidation of the functions of genes central to diterpene metabolism in tobacco trichomes using posttranscriptional gene silencing. Planta 216(4):686–691. https://doi.org/10.1007/s00425-002-0904-4

Wu M-L, Cui Y-C, Ge L, Cui L-P, Xu Z-C, Zhang H-Y, Wang Z-J, Zhou D, Wu S, Chen L, Cui H (2020) NbCycB2 represses Nbwo activity via a negative feedback loop in tobacco trichome development. J Exp Bot 71(6):1815–1827. https://doi.org/10.1093/jxb/erz542

Xu J, van Herwijnen ZO, Dräger DB, Sui C, Haring MA, Schuurink RC (2018) SlMYC1 regulates type VI glandular trichome formation and terpene biosynthesis in tomato glandular cells. Plant Cell 30(12):2988–3005. https://doi.org/10.1105/tpc.18.00571

Yan T, Chen M, Shen Q, Li L, Fu X, Pan Q, Tang Y, Shi P, Lv Z, Jiang W, Ma Y-n, Hao X, Sun X, Tang K (2017) HOMEODOMAIN PROTEIN 1 is required for jasmonate-mediated glandular trichome initiation in *Artemisia annua*. New Phytol 213(3):1145–1155. https://doi.org/10.1111/nph.14205

Yan T, Li L, Xie L, Chen M, Shen Q, Pan Q, Fu X, Shi P, Tang Y, Huang H, Huang Y, Huang Y, Tang K (2018) A novel HD-ZIP IV/MIXTA complex promotes glandular trichome initiation and cuticle development in *Artemisia annua*. New Phytol 218(2):567–578. https://doi.org/10.1111/nph.15005

Yang C, Li H, Zhang J, Luo Z, Gong P, Zhang C, Li J, Wang T, Zhang Y, Lu Y, Ye Z (2011) A regulatory gene induces trichome formation and embryo lethality in tomato. Proc Natl Acad Sci USA 108(29):11836–11841. https://doi.org/10.1073/pnas.1100532108

Yang C, Ye Z (2013) Trichomes as models for studying plant cell differentiation. Cell Mol Life Sci 70(11):1937–1948. https://doi.org/10.1007/s00018-012-1147-6

Yang C, Gao Y, Gao S, Yu G, Xiong C, Chang J, Li H, Ye Z (2015) Transcriptome profile analysis of cell proliferation molecular processes during multicellular trichome formation induced by tomato *Wov* gene in tobacco. BMC Genom 16(1):868. https://doi.org/10.1186/s12864-015-2099-7

Zhang F, Liu X, Zuo K, Zhang J, Sun X, Tang K (2011) Molecular cloning and characterization of a novel *Gossypium barbadense* L. *RAD*-Like gene. Plant Mol Biol Rep 29(2):324–333. https://doi.org/10.1007/s11105-010-0234-9

Zhao M, Morohashi K, Hatlestad G, Grotewold E, Lloyd A (2008) The TTG1-bHLH-MYB complex controls trichome cell fate and patterning through direct targeting of regulatory loci. Development 135(11):1991–1999. https://doi.org/10.1242/dev.016873